
Explaining time series models using frequency masking

Thea Brüsch¹ Kristoffer K. Wickstrøm² Mikkel N. Schmidt¹ Tommy S. Alstrøm¹ Robert Jenssen²

Abstract

Time series data is fundamentally important for describing many critical domains such as healthcare, finance, and climate, where explainable models are necessary for safe automated decision-making. To develop eXplainable AI (XAI) in these domains therefore implies explaining salient information in the time series. Current methods for obtaining saliency maps assumes localized information in the raw input space. In this paper, we argue that the salient information of a number of time series is more likely to be localized in the frequency domain. We propose FreqRISE, which uses masking based methods to produce explanations in the frequency and time-frequency domain, which shows the best performance across a number of tasks.

1. Introduction

With the increasing development of systems for automated decision-making based on time series in critical domains such as healthcare (Phan & Mikkelsen, 2022; Brüsch et al., 2023), finance (Giudici & Raffinetti, 2023) and climate forecasting (González-Abad et al., 2023), the demand for safe and trustworthy machine learning models is ever rising. High accuracy and explainability are both necessary components in achieving safety and trustworthiness. Deep learning models have become a popular choice to obtain high accuracy for time series tasks (Mohammadi Foumani et al., 2024), but due to their complex reasoning process they are difficult to interpret. Explainable artificial intelligence (XAI) aims to open up the black box (Samek et al., 2019).

Most advancements in the field of XAI have been made in explaining image inputs (Kim et al., 2018; Petsiuk et al.,

2019; Bach et al., 2015). Images hold the appeal of being easily interpretable by humans, making it simpler to validate model decisions by visual explanations. As such, many XAI methods provide explanations in the form of a relevance map over the input pixels. Time series do not benefit from the same properties, since they are by nature more difficult to understand (Rojat et al., 2021). While many time series models may be trained on raw time series data, the information (and thus relevance) may likely be found in a latent feature domain such as the frequency domain (Schröder et al., 2023). This challenge has only been addressed in (Vielhaben et al., 2024), where the authors use gradient-based methods to backpropagate the relevance into the frequency domain.

Masking-based methods are an important tool in XAI due to their high performance across a multitude of domains (Petsiuk et al., 2019; Crabbé & Van Der Schaar, 2021; Highton et al., 2024). Masking-based approaches evolve around learning or estimating the relevance maps by iteratively applying binary masks to the input and measuring the resulting change in the output. Especially optimization-based masking approaches have shown great promise for time series data (Crabbé & Van Der Schaar, 2021; Enguehard, 2023; Liu et al., 2024). In optimization-based masking approaches, the relevance is learned by posing an objective that maximizes the number of masked out features in the input, while simultaneously minimizing the change in the model output (Fong et al., 2019). The mask is optimized via gradient descent through the model and the mask generating function. These methods can be difficult to use due to hyper-parameter tuning. Additionally, they suffer from the significant drawback of requiring access to the model gradients.

Alternatively, model-agnostic methods require only access to the input and output of the network and are easily adaptable to a multitude of network architectures. Prominent model-agnostic methods are also based on masking and involve estimating the relevance via Monte Carlo sampling. This category includes RISE (Petsiuk et al., 2019) and RELAX (Wickstrøm et al., 2023). The sampling based methods have a few clear advantages: they do not require any complex optimization techniques, and we can directly constrain the sampling space to ensure compatibility with our data. While these methods have been successfully applied for time series (Mercier et al., 2022; Fedele et al., 2022), no

¹Department of Applied Mathematics and Computer Science, Technical University of Denmark, Richard Petersens Plads 324, 2800 Kgs. Lyngby, Denmark ²Department of Physics and Technology, UiT The Arctic University of Norway, Hansine Hansens veg 18, 9037 Tromsø, Norway. Correspondence to: Thea Brüsch <theb@dtu.dk>.

Submitted to the Next Generation of AI Safety workshop at the 41st International Conference on Machine Learning, Vienna, Austria. PMLR 235, 2024. Copyright 2024 by the author(s).

previous work in this category has focused on providing relevances in another domain than the input domain.

In this paper, we take inspiration from RISE and propose the first approach for masking-based XAI in the frequency domain of time series, FreqRISE. We:

- Propose FreqRISE, the first masking-based approach for providing relevance maps in the frequency domain.
- Provide a comprehensive evaluation of our proposed approach across several datasets and tasks.
- Show that masking-based relevance maps in the frequency and time-frequency domain outperform competing methods across several metrics.

2. Masking based explanations

Here, we present a new method for transforming masks between domains (Section 2.1) and use this new method to create FreqRISE (Section 2.2), the first masking-based XAI method operating in the frequency domain of time series.

2.1. Masking in a dual domain

While many time series models are trained directly on the raw time series data, the time domain is often insufficient for providing complete explanations (Schröder et al., 2023). This is due to most XAI methods being build on the assumption that the explanations are *localized* and *sparse*. However, if two classes are characterized by e.g. their frequency content, this information is neither localized nor sparse in the time domain. We, therefore, propose transforming the signals in to a domain where the information is assumed to be localized and sparse and to provide the explanations in this domain.

Our aim is to explain the black box model f that outputs the class probabilities $\mathbf{y} \in \mathbb{R}^C$ from a time series input $\mathbf{X} \in \mathbb{R}^{V \times T}$, where V is the number of input variables and T is the length of the time series. Traditional masking-based methods use masks $\mathbf{M} \in [0, 1]^{V \times T}$, to mask out features in the input space through elementwise multiplication, $\hat{\mathbf{X}} = \mathbf{X} \odot \mathbf{M}$ and observe the resulting changes in the model output:

$$\hat{\mathbf{y}} = f(\hat{\mathbf{X}}). \quad (1)$$

The result is therefore a relevance map in the input domain.

Instead, assume an invertible mapping into the domain of interest, $g : \mathbf{X}^T \rightarrow \mathbf{X}^S$. We can formulate an alternative masking-based approach, where the masks are applied in the new domain, S , after which the input is transformed back into the time domain, T . One example of such mapping is the discrete Fourier transform (DFT), which maps the signal into the frequency domain, $\mathbf{X}^S \in \mathbb{C}^{V \times F}$. We can then

apply masks $\mathbf{M}^S \in [0, 1]^{V \times F}$ in the frequency domain obtain the outputs through the inverse mapping:

$$\hat{\mathbf{X}} = g^{-1} \left(g(\mathbf{X}) \odot \mathbf{M}^S \right). \quad (2)$$

We can then use (1) to obtain the changes in the model output resulting from the mask.

In this paper, we focus on the frequency domain and the time-frequency domain, obtained through the DFT and the short-time DFT (STDFT). However, the formulation can be extended to other invertible mappings.

2.2. FreqRISE

A prominent masking-based framework is RISE (Petsiuk et al., 2019). RISE assumes that the masks M are sampled from a distribution D . RISE then estimates the relevance, $R_{c,v,t}$, of class c for a point in input space, $X_{v,t}$, as the expected value of $\hat{\mathbf{y}}_c$ (obtained using (1)) conditioned on $M_{v,t} = 1$, i.e. that the point is observed:

$$\mathbf{R} = \mathbb{E}_M[\hat{\mathbf{y}} \cdot \mathbf{M}]. \quad (3)$$

For a high accuracy classifier, we expect $\hat{\mathbf{y}}$ to be high when important time points are not masked out. In practice, we can estimate the relevance using Monte Carlo sampling. We produce N masks and estimate the expected value as a weighted sum, normalized by the expectation over the masks:

$$\hat{\mathbf{R}} = \frac{1}{N \cdot \mathbb{E}[M]} \sum_i^N \hat{\mathbf{y}} \cdot \mathbf{M}_i. \quad (4)$$

In this work, we deal with univariate time series, i.e. $V = 1$, however the methods can be extended to multivariate cases.

We combine the RISE framework with our proposed frequency and time-frequency masking and call our method FreqRISE.

3. Experimental setup

We conduct experiments on two datasets: the synthetic dataset presented in (Vielhaben et al., 2024) and AudioM-NIST (Becker et al., 2024).

3.1. Synthetic data

We use the same synthetic dataset as in (Vielhaben et al., 2024). The dataset is specifically designed to have the salient information in the frequency domain and therefore allows to test the localization ability of the XAI methods. Each datapoint is created as a sum over M sinusoids, where $M \sim \mathcal{U}(10, 50)$:

$$X_t = \sum_j^M a_j \sin \left(\frac{2\pi t}{Tk_j} + \psi_j \right) + \sigma \epsilon. \quad (5)$$

We set all $a_j = 1$, randomly sample the phase $\psi_j \sim \mathcal{U}(0, 2\pi)$, and add noise $\epsilon \sim \mathcal{N}(0, 1)$ with standard deviation σ . The length of the signals is set to $T = 2560$ and all frequency components are sampled as integer values within the range $k_j \sim \mathcal{U}\{1, 59\}$. We train the models to detect a combination of frequencies, $k^* \in \{5, 16, 32, 53\}$ from the time series signal. The classes are created from the powerset of k^* and we therefore have 16 classes. Figure 1 shows a sample from the dataset. We train a 4-layer

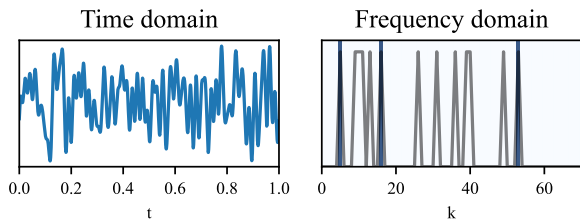


Figure 1. A sample from the synthetic dataset with salient features at $k = \{5, 16, 53\}$ marked in blue in the frequency domain.

multilayer perceptron (MLP) with a hidden size of 64 on two different versions of the raw time series: one with noise level $\sigma = 0.01$ and one with $\sigma = 0.8$. In both cases, we use 10^5 samples for training. We test the models on a test set of size 1000 with no noise. Both models achieve an accuracy of 100%.

We use FreqRISE to compute relevance maps. We use the one-sided DFT to transform the signals to the frequency domain and sample binary masks, zeroing out single frequencies with $p = 0.5$ from a Bernoulli distribution. We use $N = 3000$ masks to obtain the relevance maps.

3.2. AudioMNIST

AudioMNIST is a dataset consisting of 30,000 audio recordings of spoken digits (0-9) repeated 50 times for each of the 60 speakers (12 female/48 male) (Becker et al., 2024). We follow (Becker et al., 2024) and downsample all signals to 8kHz and zero-pad all windows to 8000 samples.

We use the same 1D convolutional architecture as in (Becker et al., 2024) on the raw time series and train two versions: one trained for predicting the spoken digit and one trained to predict the gender of the speaker. We expect the salient information for the gender task and digit to be localized in the frequency domain and time-frequency domain, respectively. We obtain an accuracy of 96.9% on the digit classification and 98.6% for the gender task.

We use FreqRISE to compute relevance maps in the frequency and time-frequency domains and standard RISE in the time domain. We use 1000 data points from the gender and digit test sets respectively for testing the explanation methods. All relevance maps for AudioMNIST are esti-

mated using $N = 20,000$ samples. All masks are sampled from a Bernoulli distribution on a lower dimensional grid and linearly interpolated to create smooth masks. When computing the (Freq)RISE relevance maps, we use the logits prior to the softmax activation, since these show higher sensitivity to changes in the input.

We use the one-sided DFT to transform the signals to the frequency domain. We sample binary masks of size 200 with $p = 0.5$ and interpolate to size $F = 4001$. In the time-frequency domain, we use the one-sided STDFT with a Hanning window of size 455 and an overlap of 420 samples between subsequent windows following (Becker et al., 2024). The binary masks are sampled as grids of size 25×25 with $p = 0.5$. Finally, in the time domain, we sample binary masks of size 200 with $p = 0.5$ and interpolate to size $T = 8000$.

3.3. Baselines

As baselines, we use Integrated Gradients (IG) (Sundararajan et al., 2017) and Layer-wise Relevance Propagation (LRP) (Bach et al., 2015). When computing relevance maps in the frequency and time-frequency domains, we follow (Vielhaben et al., 2024) and equip the models with virtual inspection layers, which map the input into the relevant domains. Due to relevance conservation, we are restricted to using rectangular, non-overlapping windows for the STDFT. We therefore use rectangular windows of size 455 with no overlap.

3.4. Quantitative evaluation

Due to the lack of ground truth explanations (Hedström et al., 2023), quantitative evaluation for XAI is performed by measuring desirable properties (Hedström et al., 2023). Below we describe three such desirable properties that we use to quantify the quality of the relevance maps.

Localization: Localization scores are widely used to evaluate if explanations are co-located with a region of interest (Wickstrøm et al., 2023; Crabbé & Van Der Schaar, 2021). For the synthetic data, we know the ground truth explanations and can therefore use localization metrics to evaluate the methods. We use the *relevance rank accuracy* (Arras et al., 2022). Assuming a ground truth mask, GT , of size K and a relevance map \hat{R} , we take the K points with the highest relevance. We then count how many of these values coincide with the positions in the ground truth mask. Formally, for $P_{topK} = \{p_1, p_2, \dots, p_K | \hat{R}_{p_1} > \hat{R}_{p_2} > \dots > \hat{R}_{p_K}\}$, i.e. p denotes the position, we compute:

$$\text{Relevance rank accuracy} = \frac{|P_{topK} \cap GT|}{|GT|}. \quad (6)$$

Faithfulness: Faithfulness measures to what degree an ex-

planation follows the predictive behaviour of the model and is a widely used measure for quantifying quality of explanations (Vielhaben et al., 2024; Liu et al., 2024). We follow prior works (Vielhaben et al., 2024; Crabbé & Van Der Schaar, 2021) and compute faithfulness as follows. Given a relevance map, \hat{R} , we iteratively remove the 5%, 10%, ..., 95% most important features by setting the signal value to 0. We then evaluate the model performance as the mean probability of the true class and plot it to produce deletion plots. Finally, we compute the area-under-the-curve to produce our final faithfulness metric.

Complexity: Finally, we evaluate the complexity of the explanation as an estimate for the informativeness (Bhatt et al., 2021). The complexity is estimated as the Shannon entropy of the relevance maps.

4. Results

4.1. Synthetic data results

Table 1 shows the localization and complexity scores across the different methods for both the model trained on the low noise and the noisy datasets. The results on the low noise model show that all XAI methods perform approximately equal on the localization score, while IG and LRP yield relevance maps with substantially lower complexity scores compared to FreqRISE. However, when we move to the noisy model, the localization score of FreqRISE is unchanged, whereas both IG and LRP have much lower performance. The complexity of the IG and LRP relevance maps is slightly higher on the noisy model, while the complexity of the FreqRISE is unchanged. An example of the computed relevance maps is shown in the appendix.

Table 1. Localization (L) and complexity (C) on the synthetic data.

| | Low noise | | Noisy | |
|----------|------------------|--------------------|------------------|--------------------|
| | L (\uparrow) | C (\downarrow) | L (\uparrow) | C (\downarrow) |
| IG | 99.1% | 1.10 | 52.4% | 1.96 |
| LRP | 99.1% | 1.11 | 63.8% | 1.34 |
| FreqRISE | 100.0% | 7.09 | 100.0% | 7.09 |

4.2. AudioMNIST results

Following the procedure described in Section 3.4, we initially compute the faithfulness results. Figure 2 shows the deletion plots for the digit classification task in the frequency and time-frequency domain. We have also included two additional baselines, namely randomly deleting features and deleting features based on their amplitude. In both domains, the mean true class probability quickly drops. After dropping only 15% of the features, FreqRISE has a mean true class probability of 0.206 in the time-frequency domain

and 0.194 in the frequency domain. After this, the value continues to drop with features being removed.

Figure 3 shows the same results for the gender classification task. Here, the mean true class probability using FreqRISE is 0.434 after dropping only 5% of the features in the frequency domain, while the same value in the time-frequency domain is 0.836. The other methods show a different trend in time-frequency domain, but the results show that FreqRISE has a more difficult time masking out relevant features in the time-frequency domain.

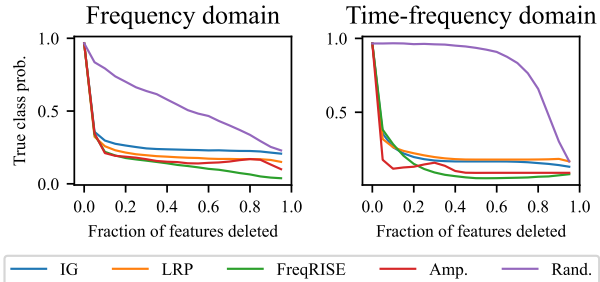


Figure 2. AudioMNIST: Deletion plots for the digit task.

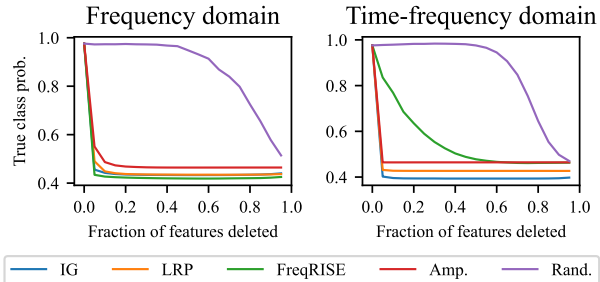


Figure 3. AudioMNIST: Deletion plots for the gender task.

Table 2. AudioMNIST: Faithfulness of explanations in the time (T), frequency (F) and time-frequency (TF) domain.

| | Digit (\downarrow) | | | Gender (\downarrow) | | |
|------------|------------------------|-------------|-------------|-------------------------|-------------|-------------|
| | T | F | TF | T | F | TF |
| IG | .183 | .251 | .194 | .470 | .428 | .389 |
| LRP | .168 | .204 | .209 | .401 | .431 | .420 |
| (Freq)RISE | .212 | .147 | .125 | .399 | .414 | .525 |

In Table 2, the faithfulness scores are shown for both models in all three domains. We notice that in the time domain, RISE performs either worse or equivalently compared to LRP. However, when we move to the frequency domain, the faithfulness scores are lowest for FreqRISE in both cases. Finally, when we look at the time-frequency domain, the faithfulness score increases for FreqRISE on the gender

task, while it decreases on the digit task. These results indicate that the information is sparser for the digit task in the time-frequency domain.

Table 3 shows the complexity scores across all methods, domains and tasks. Again, it is clear that the complexity of the masking based models is higher compared to the remaining methods.

Table 3. AudioMNIST: Complexity scores for explanations in the time (T), frequency (F) and time-frequency (TF) domains.

| | Digit (\downarrow) | | | Gender (\downarrow) | | |
|------------|------------------------|-------------|-------------|-------------------------|-------------|-------------|
| | T | F | TF | T | F | TF |
| IG | 6.93 | 6.41 | 5.26 | 6.57 | 4.74 | 4.04 |
| LRP | 6.88 | 5.84 | 4.67 | 6.78 | 5.16 | 4.16 |
| (Freq)RISE | 8.86 | 8.17 | 10.82 | 8.86 | 8.01 | 10.78 |

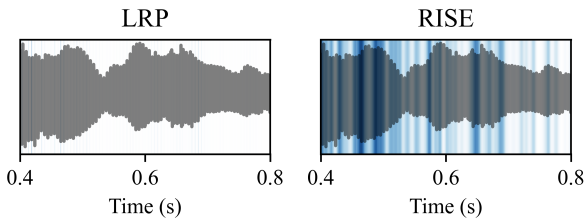


Figure 4. AudioMNIST: Gender classification, relevance map in the time domain.

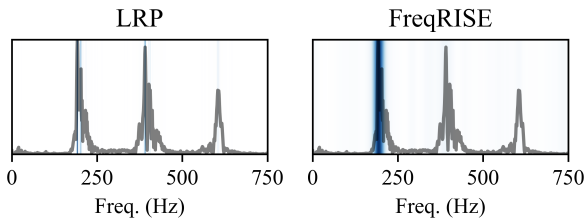


Figure 5. AudioMNIST: Gender classification, relevance map in the frequency domain.

Figure 4 shows an example of relevance maps computed in the time domain on the gender classification task. Figure 5 shows the same sample in the frequency domain. The sample is from a female speaker and the model correctly predicts the class. We see that LRP has a very sparse but scattered signal in the time domain, while RISE appears very noisy. Moving to the frequency domain, the relevance is much more localized, with FreqRISE putting most emphasis on the fundamental frequency, while LRP also focuses on the harmonics. The fundamental frequency is known to be discriminative of gender (Baken & Orlikoff, 2000).

Figure 6 shows the relevance map computed using FreqRISE in the time-frequency domain for the digit task. The spoken and predicted digit is 9. The relevance map shows

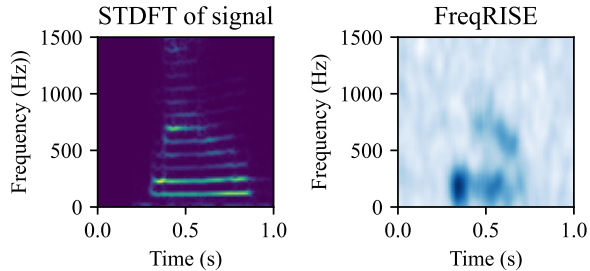


Figure 6. AudioMNIST: Digit classification, relevance map in the time-frequency domain.

that most relevance is put just at the beginning of the signal. However, around $t = 0.5$, there are two distinct patterns emerging along the frequency axis. This shows the benefit of having both the time and frequency component when computing relevance maps for the digit task.

5. Discussion and conclusion

Time series data is inherently difficult to interpret, due to the complex patterns of the signals. Therefore, providing relevance maps in a domain where information is sparser and more easily interpretable is desirable. We therefore proposed FreqRISE, which computes relevance maps in the frequency and time-frequency domains using model-agnostic masking methods. Vielhaben et al. (2024) previously produced relevance maps in these domains using gradient based methods, which are model-dependent, limiting the usability in cases where model gradients are not available.

RISE and FreqRISE consistently yield high complexity scores. While LRP and IG are able to assign zero relevance, this is generally not the case for Freq(RISE). This is, however, not necessarily indicative of the perceptual quality of the relevance maps. The entropy could e.g. be reduced through postprocessing of relevance maps.

We used a synthetic dataset with known salient features in the frequency domain to compute localization scores. In the low noise setting, FreqRISE gave slightly higher accuracy in identifying the correct frequency components. However, when testing in the high noise setting, FreqRISE outperformed the two baseline methods by a large margin (100% vs. 64%). These results indicate that FreqRISE is more robust in correctly identifying salient features in the frequency domain.

On AudioMNIST, we measured the faithfulness of all methods across three domains. RISE performed either slightly worse or similar to the baseline methods in the time domain. However, in the frequency domain FreqRISE gave the best faithfulness scores. In the time-frequency domain,

FreqRISE gave the best performance on the digit task, but the worst performance on the gender task. This leads us to believe that FreqRISE is most suitable for providing explanations in domains where the information is assumed to be sparse. While the same information can theoretically be found in e.g. the time domain, the intricacy of the patterns would require more advanced masking schemes to identify the same patterns.

We believe that XAI methods that can provide frequency and time-frequency relevance maps are important components in ensuring safe and trustworthy time series models.

Impact Statement

This paper presents work whose goal is to advance the field of explainable AI. Explainable AI is a necessary tool in obtaining safe and trustworthy models. However, if the explanations are not correct, they can potentially create a false sense of confidence in the models and cause errors in critical domains.

References

- Arras, L., Osman, A., and Samek, W. CLEVR-XAI: A benchmark dataset for the ground truth evaluation of neural network explanations. *Information Fusion*, 81:14–40, 2022.
- Bach, S., Binder, A., Montavon, G., Klauschen, F., Müller, K. R., and Samek, W. On pixel-wise explanations for non-linear classifier decisions by layer-wise relevance propagation. *Plos One*, 10(7):0130140, 2015.
- Baken, R. and Orlikoff, R. *Clinical Measurement of Speech and Voice*. Speech Science. Singular Thomson Learning, 2000.
- Becker, S., Vielhaben, J., Ackermann, M., Müller, K.-R., Lapuschkin, S., and Samek, W. AudioMNIST: Exploring explainable artificial intelligence for audio analysis on a simple benchmark. *Journal of the Franklin Institute*, 361(1):418–428, 2024.
- Bhatt, U., Weller, A., and Moura, J. M. F. Evaluating and aggregating feature-based model explanations. In *Proceedings of the Twenty-Ninth International Joint Conference on Artificial Intelligence, IJCAI’20*, 2021.
- Brüsch, T., Schmidt, M. N., and Alstrøm, T. S. Multi-view self-supervised learning for multivariate variable-channel time series. In *2023 IEEE 33rd International Workshop on Machine Learning for Signal Processing (MLSP)*, pp. 1–6, 2023.
- Cooper, J., Arandjelović, O., and Harrison, D. J. Believe the hype: Hierarchical perturbation for fast, robust, and model-agnostic saliency mapping. *Pattern Recogn.*, 129(C), sep 2022.
- Crabbé, J. and Van Der Schaar, M. Explaining time series predictions with dynamic masks. In Meila, M. and Zhang, T. (eds.), *Proceedings of the 38th International Conference on Machine Learning*, volume 139 of *Proceedings of Machine Learning Research*, pp. 2166–2177. PMLR, 18–24 Jul 2021.
- Enguehard, J. Learning perturbations to explain time series predictions. In Krause, A., Brunskill, E., Cho, K., Engelhardt, B., Sabato, S., and Scarlett, J. (eds.), *Proceedings of the 40th International Conference on Machine Learning*, volume 202 of *Proceedings of Machine Learning Research*, pp. 9329–9342. PMLR, 23–29 Jul 2023.
- Fedele, A., Guidotti, R., and Pedreschi, D. Explaining siamese networks in few-shot learning for audio data. *Lecture Notes in Computer Science (including Subseries Lecture Notes in Artificial Intelligence and Lecture Notes in Bioinformatics)*, 13601:509–524, 2022.
- Fong, R., Patrick, M., and Vedaldi, A. Understanding deep networks via extremal perturbations and smooth masks. *2019 IEEE/CVF International Conference on Computer Vision (iccv)*, pp. 2950–2958, 2019.
- Giudici, P. and Raffinetti, E. SAFE artificial intelligence in finance. *Finance Research Letters*, 56:104088, 2023.
- González-Abad, J., Baño-Medina, J., and Gutiérrez, J. M. Using explainability to inform statistical downscaling based on deep learning beyond standard validation approaches. *Journal of Advances in Modeling Earth Systems*, 15(11), 2023.
- Hedström, A., Weber, L., Krakowczyk, D., Bareeva, D., Motzkus, F., Samek, W., Lapuschkin, S., and Höhne, M. M. M. Quantus: An explainable ai toolkit for responsible evaluation of neural network explanations and beyond. *Journal of Machine Learning Research*, 24(34): 1–11, 2023.
- Hedström, A., Bommer, P., Wickstrøm, K. K., Samek, W., Lapuschkin, S., and Höhne, M. M. C. The meta-evaluation problem in explainable ai: Identifying reliable estimators with metaquantus. *Transactions on Machine Learning Research*, 2023. ISSN 2835-8856.
- Highton, J., Chong, Q. Z., Crawley, R., Schnabel, J. A., and Bhatia, K. K. Evaluation of randomized input sampling for explanation (rise) for 3d xai - proof of concept for black-box brain-hemorrhage classification. In Su, R., Zhang, Y.-D., and Frangi, A. F. (eds.), *Proceedings of 2023 International Conference on Medical Imaging and Computer-Aided Diagnosis (MICAD 2023)*, pp. 41–51, Singapore, 2024. Springer Nature Singapore.

- Kim, B., Wattenberg, M., Gilmer, J., Cai, C., Wexler, J., Viegas, F., and sayres, R. Interpretability beyond feature attribution: Quantitative testing with concept activation vectors (TCAV). In Dy, J. and Krause, A. (eds.), *Proceedings of the 35th International Conference on Machine Learning*, volume 80 of *Proceedings of Machine Learning Research*, pp. 2668–2677. PMLR, 10–15 Jul 2018.
- Liu, Z., ZHANG, Y., Wang, T., Wang, Z., Luo, D., Du, M., Wu, M., Wang, Y., Chen, C., Fan, L., and Wen, Q. Explaining time series via contrastive and locally sparse perturbations. In *The Twelfth International Conference on Learning Representations*, 2024.
- Mercier, D., Dengel, A., and Ahmed, S. TimeREISE: Time series randomized evolving input sample explanation. *Sensors*, 22(11):4084, 2022.
- Mohammadi Foumani, N., Miller, L., Tan, C. W., Webb, G. I., Forestier, G., and Salehi, M. Deep learning for time series classification and extrinsic regression: A current survey. *ACM Comput. Surv.*, 56(9), apr 2024.
- Petsiuk, V., Das, A., and Saenko, K. RISE: Randomized input sampling for explanation of black-box models. *British Machine Vision Conference 2018, Bmvc 2018*, 2019.
- Phan, H. and Mikkelsen, K. Automatic sleep staging of eeg signals: recent development, challenges, and future directions. *Physiological Measurement*, 43(4):04TR01, apr 2022.
- Rojat, T., Puget, R., Filliat, D., Del Ser, J., Gelin, R., and Díaz-Rodríguez, N. Explainable artificial intelligence (XAI) on timeseries data: A survey. 2021.
- Samek, W., Montavon, G., Vedaldi, A., Hansen, L. K., and Müller, K.-R. *Explainable AI: interpreting, explaining and visualizing deep learning*, volume 11700. Springer Nature, 2019.
- Schröder, M., Zamanian, A., and Ahmidi, N. Post-hoc saliency methods fail to capture latent feature importance in time series data. *Lecture Notes in Computer Science (including Subseries Lecture Notes in Artificial Intelligence and Lecture Notes in Bioinformatics)*, 13932:106–121, 2023.
- Sundararajan, M., Taly, A., and Yan, Q. Axiomatic attribution for deep networks. In Precup, D. and Teh, Y. W. (eds.), *Proceedings of the 34th International Conference on Machine Learning*, volume 70 of *Proceedings of Machine Learning Research*, pp. 3319–3328. PMLR, 06–11 Aug 2017.
- Vielhaben, J., Lapuschkin, S., Montavon, G., and Samek, W. Explainable AI for time series via Virtual Inspection Layers. *Pattern Recognition*, 150:110309, 2024.
- Wickstrøm, K. K., Trosten, D. J., Løkse, S., Boubekki, A., Mikalsen, K. O., Kampffmeyer, M. C., and Jenssen, R. RELAX: Representation learning explainability. *International Journal of Computer Vision*, 131(6):1584–1610, 2023.

A. Design choices for FreqRISE

As with other masking-based approaches, computing the relevance maps for FreqRISE involves choosing a number of hyper-parameters, i.e. the size of the grid in which to sample binary masks, the probability p with which a bin is chosen, and the number of masks. As of now, there is no principled way to choose either and we have heuristically chosen the hyper-parameters based on qualitative assessment on a few validation samples. A more systematic approach, would be to tune the parameters on a validation set by choosing a few metrics, such as faithfulness and complexity.

For AudioMNIST, FreqRISE needs a large number of masks to converge ($N = 20,000$). We found that when using fewer masks, the method still finds the relevant bits, but sorting out the irrelevant bits of the signal requires more masks. Wickström et al. (2023) presented theoretical results on computing the number of masks and found that $N = 3,000$ should yield results with a low error. It would be interesting to investigate convergence properties for our datasets in light of the theoretical results.

Additionally, Mercier et al. (2022) propose TimeREISE which uses a multiple mask sizes and sampling probabilities to compute the relevance maps for each time series. Finally, Cooper et al. (2022) apply RISE to images and propose a hierarchical systematic mapping to reduce the number of masks. Both of these avenues could be interesting to explore when masking in the frequency domain.

B. Results on synthetic data

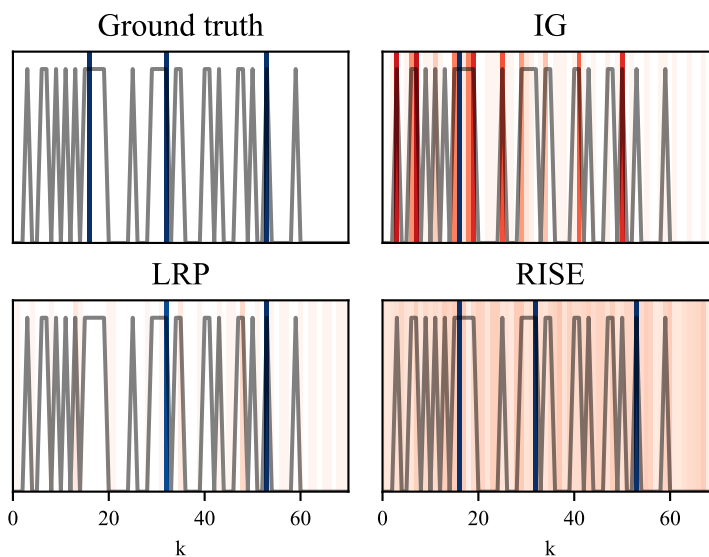


Figure 7. Synthetic data: Relevance maps from the noisy model using each method along with the ground truth for a sample in dataset.